MIT Department of Physics

Undergraduate Program

PHYSICS UNDERGRADUATE THESIS TITLE PAGE

The cover of your thesis should read:

Salty Development of an Optical Photoresist

Adam Chao

Submitted to the Department of Physics in partial fulfillment of the Requirements for the Degree of

BACHELOR OF SCIENCE

at the

MASSACHUSETTS INSTITUTE OF TECHNOLOGY
[June 2008]
May. 2008

© 2008 Adam Chao
All Rights Reserved

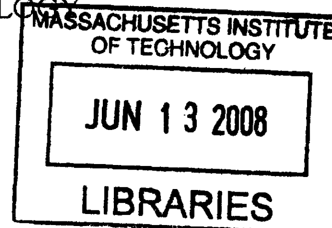

The author hereby grants to MIT permission to reproduce and to distribute publicly paper and electronic copies of this thesis document in whole or in part.

Signature of Author

Department of Physics
(Date of signature)

Certified by

"Supervisor's Name"
Thesis Supervisor, Department of Physics

(If supervisor is not in Physics, list correct department.) Department of EECS

"Co-Supervisor's Name"

Accepted by

Professor David E. Pritchard
Senior Thesis Coordinator, Department of Physics

Salty Development of an Optical Photoresist

A. Chao

Dept. of Physics

MIT, 77 Massachusetts Ave.

Cambridge, MA 02139-4307

Abstract

In this series of experiments, we add salt to a photoresist developer and observe the effect on photoresist contrast. In order to measure contrast, we designed an anti-reflection coating stack to reduce reflections between the photomask and the photoresist. After development, we observe that for 400 nm exposures of photoresist PS4 that there is no significant change in contrast with salty development, however, for samples exposed at 220 nm, there is contrast enhancement. However, it is not clear how much of the contrast enhancement for the 220 nm samples was due to the shorter wavelength, and how much was due to a different developer concentration versus the 400 nm samples. That being said, we hypothesize that the observed contrast enhancement is due to differences in photoresist cross-linking due to the different wavelength exposures.

1 Introduction

The semiconductor industry requires increasingly smaller microelectronic circuits in order to improve performance. This requires improvements in lithography and pattern generation. One important aspect of photolithography is photoresist contrast, which helps determines the clarity and resolution of micro-lithographic patterns. Previous work shows that the contrast of electron-beam resists is improved by adding salt to developer [10]. Therefore, we sought to determine whether the addition of salt to developer would increase the contrast of optical photoresists, operating in the 200-400 nm wavelength region. The discovery of contrast-enhancement through salty development has the possibility of improving photolithographic patterning, aiding the microelectronics industry in creating smaller, faster devices.

2 Basics of Photolithography

Modern semiconductor patterning makes heavy use of photolithography to write micro-sized patterns needed for complex circuits. In microscale manufacturing, four basic processes are utilized: layering, patterning, doping and heat treatments [11, 74]. Layering involves depositing or growing a a thin layer of material on the substrate, such as growing SiO_2 on silicon, or electroplating metals on a wafer. Patterning involves removing certain portions of the layer, to create a pattern of material that will form the basis for the electronic circuit or microscale device. This is done through lithography, using light to pattern a photoactive chemical, which in turn transfers that pattern to the underlying material. Doping involves putting trace chemicals into a material to alter its properties, such as implanting ions into a substrate to increase the density of electrons. Finally, heat treatments simply heat up the wafer, allowing diffusion of dopants, or evaporation of solvents, etc.

Clearly, one of the most important tasks in microfabrication is patterning, which is accomplished through lithography. Photolithography uses a light-sensitive material, called a photoresist, that is deposited onto a substrate. Light is then passed through a mask, exposing the photoresist and transferring a pattern onto it. There are two main types of photoresists. A positive photoresist is one where exposure to light increases the solubility of the resist. A negative resist is one where exposure to light decreases solubility. After exposure, the resist is developed in a solvent, with the more soluble portions dissolving away. Afterward, some type of etching process is typically performed on the substrate. For instance, a substrate of SiO_2 might be etched with HF acid. During the etching, the remaining photoresist protects the underlying substrate, allowing the transfer of photolithographic patterns into the substrate. Finally, after etching, the remaining photoresist is removed, allowing further processes on the sample.

There are two primary types of photolithography, contact and projection. Projection lithography occurs in the far-field, in the Fraunhofer diffraction regime. The ultimate resolution in this regime is governed by the Raleigh criterion of

$$R = k_1 \frac{\lambda}{NA} \tag{1}$$

Where k_1 is around 1 and NA is the numerical aperture, defined as NA = $n\sin(\theta)$ [1]. With projection lithography, patterns can be laid down quickly onto substrates, and typically a wafer stepper is used, which basically an assembly line of wafers,

each one being exposed in turn. Commercial projection lithography typically uses wavelengths of 193 nm in order to maximize resolution and decrease feature size.

Contact lithography, and it's cousin, proximity lithography, occur in the near-field, in the Fresnel diffraction regime. In this case, the mask is either in direct contact with the substrate, or in very close proximity. Here, the ultimate resolution is

$$R = \sqrt{\lambda g} \tag{2}$$

Where g is the size of the gap between the mask and substrate [1]. Contact lithography has the benefit of being cheaper than projection lithography because it does not require expensive lenses and focusing optics. Unfortunately, contact lithography has the drawback of possible contamination of the substrate by the mask, as well as other defects introduced by the mask. These include reflections and interference patterns between the mask and substrate, which caused great problems in this particular experiment.

The previous optical equations give the maximum optical resolution, assuming perfect pattern transfer to the substrate. However, in reality, the qualities of the photoresist greatly determine how well a pattern is transferred to a substrate. This is where photoresist chemistry is involved.

The basic component of photoresists is a light or energy sensitive polymer aka photoactive compound (PAC). For a positive resist, light exposure breaks down the bonds between polymer molecules, making them more soluble in the developer solution. Many positive photoresists use a form of phenol-formaldehyde novolak resin, which becomes more soluble upon light exposure. For a negative resist, exposure results in cross-linking between polymer chains, making them relatively insoluble.

Photoresists are typically dissolved in solvents, in order to easily spin layers of resist on wafers. A typical solvent for a negative resist is xylene, a benzene derivative. After spinning, the solvent is baked off. In addition, a photoresist may contain various sensitizers and additives to tailor its specific properties.

The photoresist we used was OHKA PS4, a chemically amplified resist (CA resist). CA resists have chemical additives that increase polymerization during light exposure. CA resists typically work using a molecule called a photoacid generator. Upon excitation, photoacid generators create an acid which catalyzes polymerization. The advantage is that the acid can catalyze multiple polymer molecules, greatly increasing the light sensitivity of the photoresist. With chemically amplified resists, a postexposure bake is required; this increases the diffusion of acid molecules, aid-

ing polymerization of the resist. The downside of CA resists is that they are very susceptible to contamination, requiring careful handling.

There are several important resist properties to note. A resist's aspect ratio is the ratio of the width of a resist feature to its height; a low aspect ratio allows for tall and thin resist structures, which in some cases can be useful in wafer patterning. A resist's adhesion to the substrate is also important; in some cases, hexamethyldisilazane (HMDS) is used to allow a resist to better adhere to a surface. Resists also have a specific sensitivity, that is, the amount of energy per area (typically in joules/cm^2) to expose the resist. Lower sensitivities mean longer exposure times, which can be costly. The property known as process latitude indicates how well the resist functions even when various factors such as light dose, baking time, etc are varied.

Of course, a major resist property is how well the resist replicates optical patterns that are exposed on it. We already discussed the fundamental optical limitations to lithography, but photoresists present other problems, as well. One is the proximity effect; light diffracts around patterns in the mask, exposing portions of resist that are covered by the mask, which typically results in shrinking features [11, 286]. Another effect is subject contrast, where some light penetrates into the covered region of the resist, leaving a partially exposed region between the exposed and unexposed regions [11, 286]. Thus, to create fine features, we need a strict cutoff between the solubility of exposed resist and the solubility of unexposed resist. This is property is called photoresist contrast, and is typically given as

$$C = \frac{\partial(\mathrm{RTR})}{\partial \log(\mathrm{E})} \tag{3}$$

Where RTR is the resist thickness remaining after development and E is the dose the resist receives, measured in joules per area. Thus, photoresist contrast is an important property in creating well-defined photolithographic features.

This problem of resist contrast is not just limited to photoactive resists. Electron-beam lithography uses high energy (keV) electrons to expose a resist. The de Broglie wavelength of these electrons is typically less than a nanometer, allowing extremely high resolution lithography in the nanometer range. The downside is that electron beam systems are both slow and extremely expensive, limiting their commercial uses. The electrons in E-beam lithography have such small wavelengths that the smallest feature size is determined not by the wavelength of the electrons, but rather by other factors. Resolution can be altered by either altering the resist's electron-beam point

spread function (PSF) or by altering the resist contrast [10]. The electron-beam point spread function is a characterization of how electrons scatter in the resist. The primary electrons of the beam can knock loose electrons in the resist molecules, and both these scattered primary and secondary electrons can expose portions of resist. Altering the resist PSF can be done by altering the electron energy, as well as the resist thickness, but both of these are fairly constrained during a particular process.

3 Prior Work- Salty Development of HSQ

Thus, increasing the resolving power of a resist (both photolithographic and electron-beam) requires increasing the resist contrast. Hydrogen silsesquioxane (HSQ) is a negative resist with several beneficial properties; unfortunately, it also suffers from low contrast. An innovative method of increasing the contrast of HSQ has been achieved using the addition of salt to the developer. HSQ is developed in an alkaline solution such as tetramethylammonium hydroxide (TMAH) or sodium hydroxide (NaOH). Adding a salt such as NaCl to a sodium hydroxide developer has been shown to greatly increase the contrast of HSQ [10]. Moreover, this contrast enhancement occurs without a reduction in sensitivity. Typically, when increasing a resist's contrast, the sensitivity of the resist decreases, meaning it takes a greater exposure to fully expose the resist, naturally leading to longer exposure times. However, this does not seem to be the case with HSQ and salty development. Maximum contrast was achieved with a mixture of 1% wt. NaOH and 4% wt. NaCl [10].

As a practical illustration of resist contrast enhancement, 14 nm-pitch nested "L" structures were produced [10]. Salty development clearly shows better resolved features due to enhanced resist contrast.

Currently, it is unclear what chemical processes cause salty development to increase contrast in HSQ. It is hypothesized that the presence of an ionic species increases reaction rates, allowing both greater cross-linking between exposed regions and greater dissolution for unexposed regions [10].

4 Salty development and Photoresists

The results with HSQ motivated us to find out whether salty development enhanced the contrast of optical photoresists, not just e-beam ones. We decided to use a negative photoresist, PS4, made by Ohka in Japan. Measuring the contrast of the resist

htb

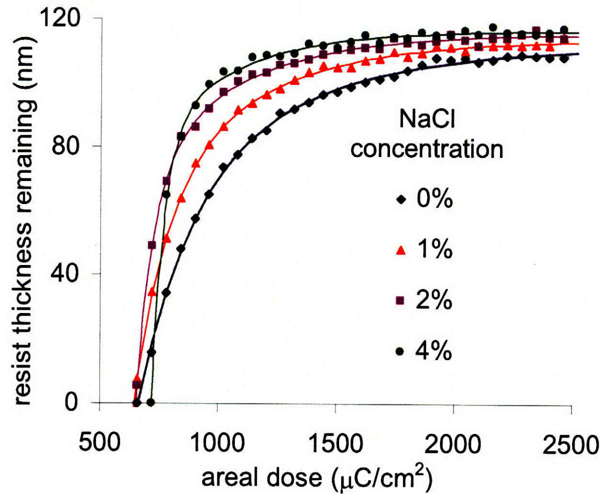

Figure 1: Shown is the increasing slope of the RTR versus dose curve for increasing NaCl concentrations, illustrating the contrast enhancement due to salty development. Reproduced with permission of [10]

requires exposing the resist for different intervals of time, and after development measuring the thickness of the remaining resist. Ideally, we would have used projection lithography in order to rule out resist contamination and other effects. However, we were limited to using the MIT Nanostructures Laboratory in Building 39, which only has contact lithography systems. We had a mask fabricated (shown in Figure 3), where each line would be isolated during exposure by covering the others with aluminum foil. Thus, we could adjust the dose individually for each line and measure its thickness using the Dektak profilometer. We spun PS4 on a silicon wafer at 1,500 RPM, which created a thickness of about 250 nm. After pre-baking for 60 seconds at 90 C, we exposed at 220 nm on the OAI machine, using the mask.

Unfortunately, after an initial test exposure, we had lines as shown in Figure 4:

Evidently, reflections were occurring between the silicon substrate, photoresist, and mask, causing interference lines. The orderly lines indicates that the mask is slightly tilted with respect to the wafer, as illustrated in Figure 5. In an effort to reduce the reflections, were tried using an anti-reflection coating, which is spun on before the PS4.

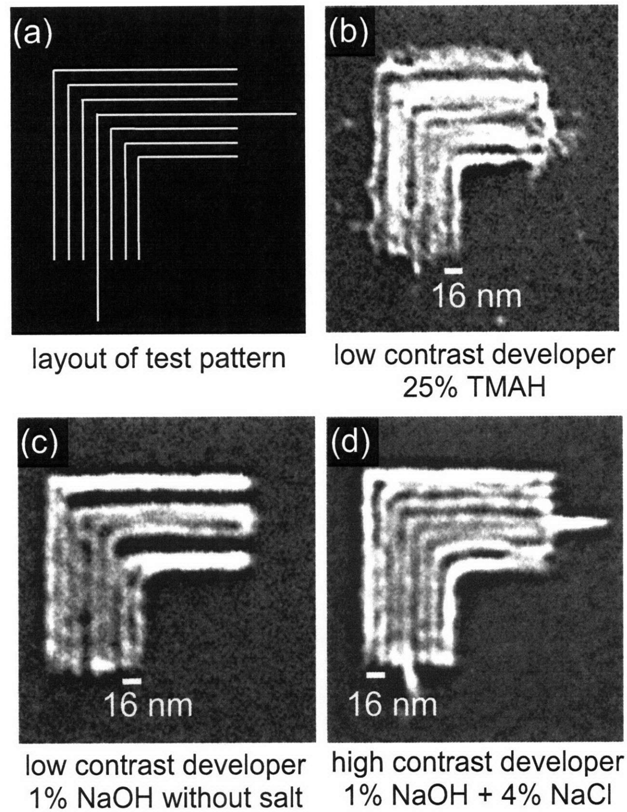

Figure 2: Lithographic structures qualitatively showing enhanced contrast through salty development. Reproduced with permission of [10]

5 Anti-reflection coatings

As shown in the previous images, in measuring the photoresist contrast of PS4, we faced a problem with interference patterns and reflections off of the mask. Our lack of a projection system necessitated contact lithography, as well. Therefore, we sought to reduce the reflections in order to obtain better results. For this reason, we used an anti-reflection coating (ARC) underneath the PS4; we used both Barli ARC and XHRIC ARC in an attempt to minimize reflections.

Beforehand, we calculated the optimal ARC thickness on the computer. The theory behind it is expressed in Kong's "Electromagnetic Wave Theory" and is as follows [5]:

If we consider an electromagnetic wave with a plane of incidence parallel to the

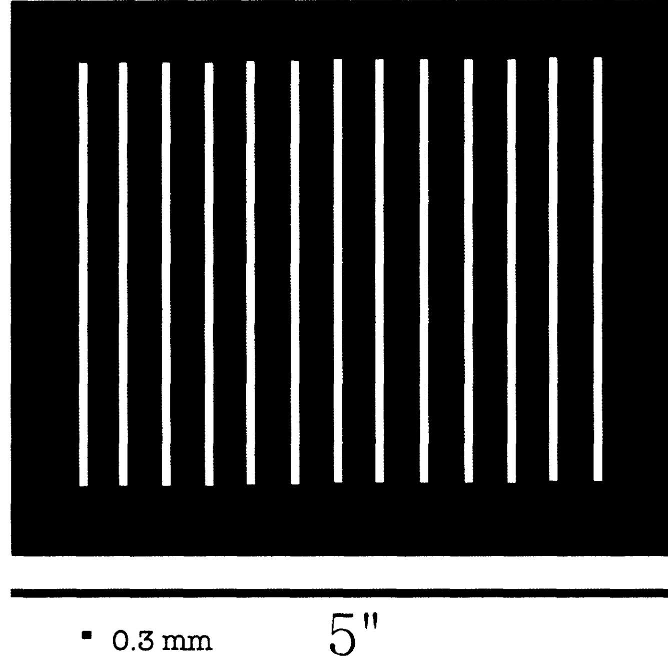

Figure 3: Design for the photomask used, white is transparent, black is opaque

x-z plane. Since all vectors are independent of y, the derivatives with respect to y drop out. The wave incident on a layered material with n regions, and boundaries between the regions located at x = -d_0, -d_1,...,-d_n. Thus Maxwell's equations in an layer l in the material are given by:

$$H_{lx} = -\frac{1}{i\omega\mu_l}\frac{\partial}{\partial z}E_{ly} \tag{4}$$

$$H_{lz} = \frac{1}{i\omega\mu_l}\frac{\partial}{\partial x}E_{ly} \tag{5}$$

$$(\frac{\partial^2}{\partial x^2} + \frac{\partial^2}{\partial z^2} + \omega^2\mu_l\epsilon_l)E_{ly} \tag{6}$$

$$E_{lx} = \frac{1}{i\omega\epsilon_l}\frac{\partial}{\partial z}H_{ly} \tag{7}$$

$$H_{lz} = -\frac{1}{i\omega\epsilon_l}\frac{\partial}{\partial x}H_{ly} \tag{8}$$

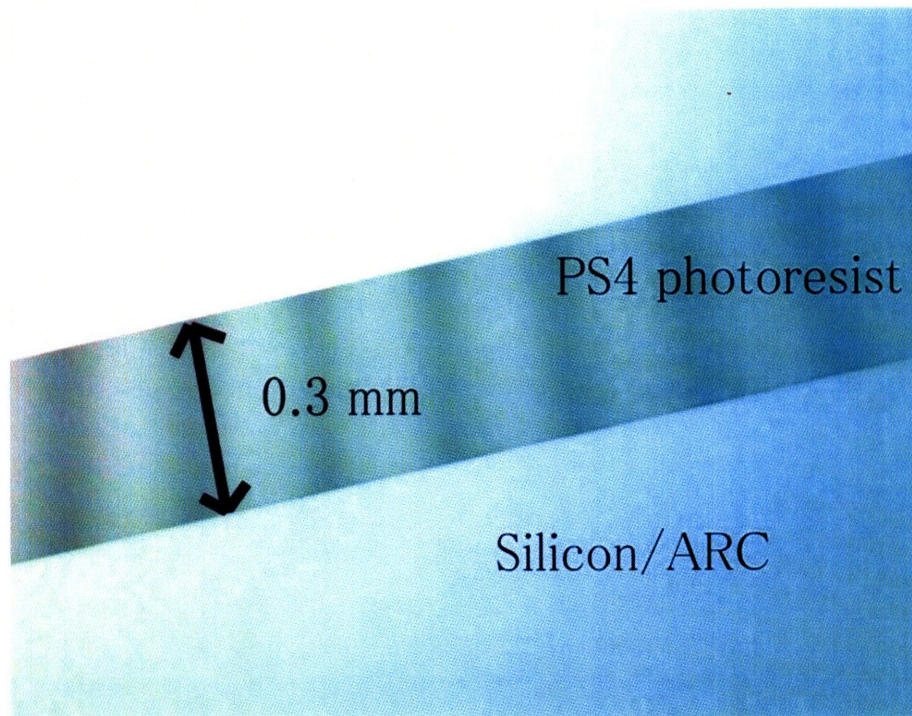

Figure 4: Optical micrograph of interference lines on photoresist due to reflections between the mask and resist

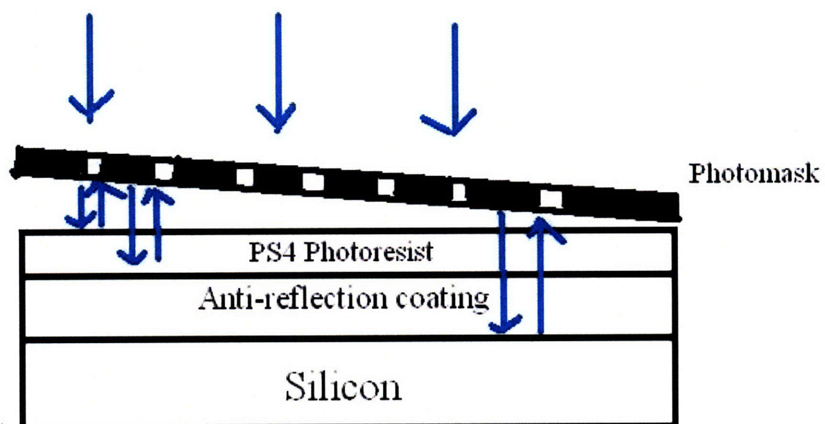

Figure 5: Sketch of how unevenness in the mask can cause interference patterns

$$(\frac{\partial^2}{\partial x^2} + \frac{\partial^2}{\partial z^2} + \omega^2 \mu_l \epsilon_l) H_{ly} \tag{9}$$

Notice the first three equations are completely decoupled from the last three. The first three represent the transverse electric (TE) waves, while the last three represent the transverse magnetic (TM) waves.

Incident TE waves on the material can be described as $E_y = E_0 e^{-ik_z z + ik_x x}$. From, this, we can describe the total incident and reflected wave:

$$E_{ly} = (A_l e^{ik_{lz} z} + B_l e^{-ik_{lz} z}) e^{ik_x x} \tag{10}$$

$$H_{lx} = -\frac{k_{lz}}{\omega \mu_l} (A_l e^{ik_{lz} z} - B_l e^{-ik_{lz} z}) e^{ik_x x} \tag{11}$$

$$H_{lz} = \frac{k_{lx}}{\omega \mu_l} (A_l e^{ik_{lz} z} + B_l e^{-ik_{lz} z}) e^{ik_x x} \tag{12}$$

Accordingly, at a boundary z = -d_l, E_y must be continuous, so that:

$$A_l e^{-ik_{lz} d_l} + B_l e^{ik_{lz} d_l} = A_{l+1} e^{-ik_{(l+1)lz} d_l} + B_{l+1} e^{ik_{(l+1)z} d_l} \tag{13}$$

In addition, H_x must be continuous, so:

$$\frac{k_{lz}}{\mu_l} (A_l e^{-ik_{lz} d_l} - B_l e^{ik_{lz} d_l}) = \frac{k_{(l+1)z}}{\mu_{l+1}} (A_{l+1} e^{-ik_{(l+1)z} d_l} - B_{l+1} e^{ik_{(l+1)z} d_l}) \tag{14}$$

For anti-reflection coating, we need to minimize the total reflection coming off of the material. Furthermore, we know that $A_0 = RE_0$, where R is the total reflection coefficient, and that $B_0 = E_0$, representing the incident wave. Thus, to find R, we need to find A_0/B_0. We can do this by using the previous equations to solve for A_l and B_l.

$$A_l e^{-ik_{lz} d_l} = \frac{1}{2}(1 + p_{l(l+1)})(A_{l+1} e^{-ik_{(l+1)z} d_l} + R_{l(l+1)} B_{l+1} e^{ik_{(l+1)z} d_l}) \tag{15}$$

$$B_l e^{ik_{lz} d_l} = \frac{1}{2}(1 + p_{l(l+1)})(R_{l(l+1)} A_{l+1} e^{-ik_{(l+1)z} d_l} + B_{l+1} e^{ik_{(l+1)z} d_l}) \tag{16}$$

Where

$$p_{l(l+1)} = \frac{\mu_l k_{(l+1)z}}{\mu_{l+1} k_{lz}} \tag{17}$$

And

$$R_{l(l+1)} = \frac{1 - p_{l(l+1)}}{1 + p_{l(l+1)}} \tag{18}$$

From this, we can get A_l/B_l:

$$\frac{A_l}{B_l} = \frac{e^{i2k_{lz}d_l}}{R_{l(l+1)}} + \frac{(1 - (1/R^2_{l(l+1)}))e^{i2(k_{(l+1)z}+k_{lz})d_l}}{(1/R_{l(l+1)})e^{i2k_{(l+1)z}d_l} + (A_{l+1}/B_{l+1})} \tag{19}$$

For our experiment, we have 3 total layers: photoresist, anti-reflection coating, and silicon. Using notation for continued fractions, this gives us:

$$R = \frac{e^{i2k_zd_0}}{R_{01}} + \frac{(1 - (1/R^2_{01}))e^{i2(k_{1z}+k_{lz})d_0}|}{(1/R_{01})e^{i2k_{1z}d_0}} + \frac{e^{i2k_{1z}d_1}}{R_{12}} + \frac{(1 - (1/R^2_{12}))e^{i2(k_{2z}+k_{2z})d_1}|}{(1/R_{12})e^{i2k_{2z}d_1}} + R_{23}e^{(2ik_{2z}d_2)}; \tag{20}$$

For the three layer stack we have, we have values for the indices of refraction for the three layers: n_{PS4}, n_{ARC}, n_{silicon}. From electromagnetism, we know that $k_l = \frac{\omega n_l}{c}$. We can also find out the thickness of the PS4 layer that is spun on. I'll elaborate a little on how this was done:

5.1 Finding Index of Refraction Values and Thicknesses

In order to find the optimal thickness of anti-reflection coating required, we need the indices of refraction for the different layers. There are several ways to find values for the index of refraction of the photoresist and anti-reflection coating. One is simply to look at the manufacturing specifications. For 351 nm (the closest to the 400 nm light we were using), n_{PS4} = 1.667 - 0.016i, n_{XHRIC} = 1.69 - 0.38i [7]. For 193 nm (the closest to 220 nm light), n_{PS4} = 1.395 - 0.747i, n_{Barli} = 1.595 - 0.442i [7]. Since silicon is widely documented, finding the index for the exact wavelengths required is easy; for 400 nm, n_{Si} = 5.632 - 0.286i [4].

We also used an ellipsometer both to measure the thickness of layers and to find the index of refraction.

Light can be polarized parallel to the plane of incidence (p-polarization) or perpendicular to the plane of incidence (s-polarization). By measuring the ratio of reflection of s-polarized to p-polarized light, one can find the amplitude change (Ψ) and the phase shift (Δ).

$$\frac{r_p}{r_s} = \tan(\Psi)\mathrm{e}^{\mathrm{i}\Delta} \tag{21}$$

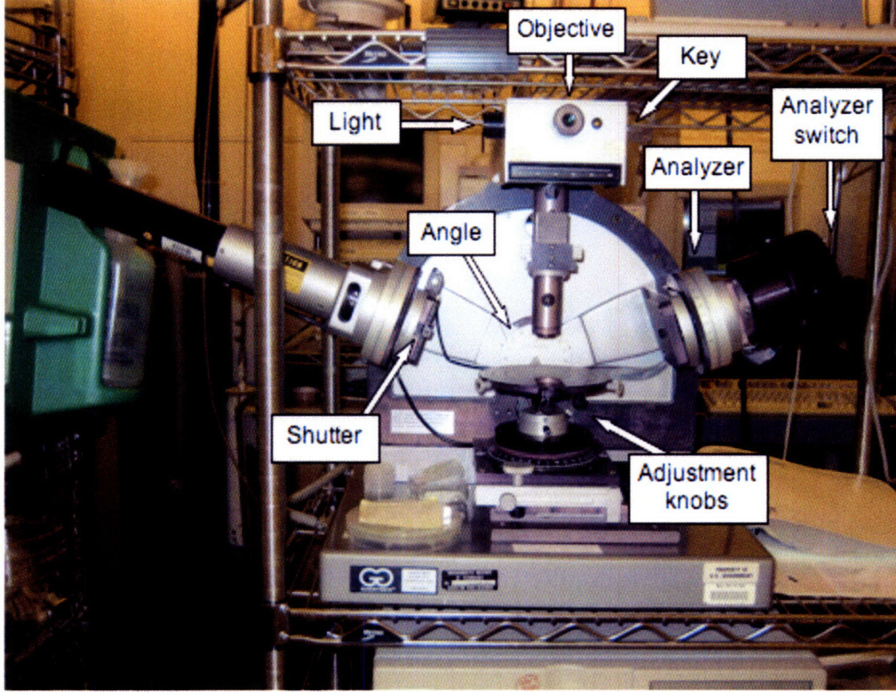

Figure 6: Photo of MIT Nanostructures Laboratory Ellipsometer [6]

With the ellipsometer we measured $n_{\mathrm{PS4}} = 1.667$, $n_{\mathrm{XHRIC}} = 1.65$, $n_{\mathrm{Barli}} = 1.7$. The discrepancy with the published numbers is probably because the ellipsometer uses a HeNe laser (632 nm), rather than the 351 nm and 193 nm that were published.

Thus, although we have data on the indices of refraction for the various materials, the index can vary with wavelength. To closer approximate the index for desired wavelengths we can use the Cauchy equation.

$$n = A + \frac{B}{\lambda^2} + \frac{C}{\lambda^4} \tag{22}$$

A quick derivation follows, as explained in Reference [3]:

We can view an atomic electron interacting with radiation as a driven oscillator, whose position is governed by the equation:

$$m\frac{d^2x}{dt^2} + m\omega_0^2 x = qE_0 e^{-i\omega t} \tag{23}$$

This has the solution:

$$x(t) = \frac{q/m}{\omega_0^2 - \omega^2} E_0 e^{-i\omega t} \tag{24}$$

The dipole moment is the real part of p = qx(t). We can generalize this to a collection of N molecules, each with f_j electrons at resonance j. The polarization is:

$$P = \frac{Nq^2}{m} (\sum_j \frac{f_j}{\omega_j^2 - \omega^2}) E \tag{25}$$

Since P = $\epsilon_0 \chi_e$E, this indicates that

$$\epsilon_r = 1 + \chi_e = 1 + \frac{Nq^2}{m\epsilon_0} (\sum_j \frac{f_j}{\omega_j^2 - \omega^2}) \tag{26}$$

The index of refraction, n = $\sqrt{\epsilon_r}$, which, assuming ω isn't near a resonance, then $\sqrt{1+\chi} = 1 + \frac{1}{2}\chi$, so that n is approximately

$$n = 1 + \frac{Nq^2}{2m\epsilon_0} (\sum_j \frac{f_j}{\omega_j^2 - \omega^2}) \tag{27}$$

We can also approximate:

$$\frac{1}{\omega_j^2 - \omega^2} = \frac{1}{\omega_j^2} (1 - \frac{\omega^2}{\omega_j^2})^{-1} =\sim \frac{1}{\omega_j^2} (1 + \frac{\omega^2}{\omega_j^2} + \frac{\omega^4}{\omega_j^4}) \tag{28}$$

Thus it's clear n can be approximated by using constants a,b,c:

$$n = a + b\omega^2 + c\omega^4 = A + \frac{B}{\lambda^2} + \frac{C}{\lambda^4} \tag{29}$$

Using the previous data on our materials at various wavelengths (193, 351, 632 nm), we can approximate the indices of refraction for the wavelengths we desire. Unfortunately, around the UV range, we start approaching various resonances, so approximating for 220 nm is problematic, but even just approximating for 400 nm exposures is useful. Moreover, the industrial specifications for XHRIC actually give us the Cauchy coefficients, so much the better. With Cauchy coefficients of A = 1.618, B = 9.08e-3 and C = 2.9e-3, we get a value for 400 nm of $n_{\text{XHRIC}} = 1.79$ [8].

For PS4, published values for 325 nm and 351 nm light are 1.681 and 1.667 respectively, which, fitted to two Cauchy coefficients correspond to A = 1.58 and B = 0.01, giving at 400 nm $n_{\text{PS4}} = 1.65$

Implementing Equation 20 in MATLAB, we obtain the reflectivity versus varying thicknesses of XHRIC at 400 nm:

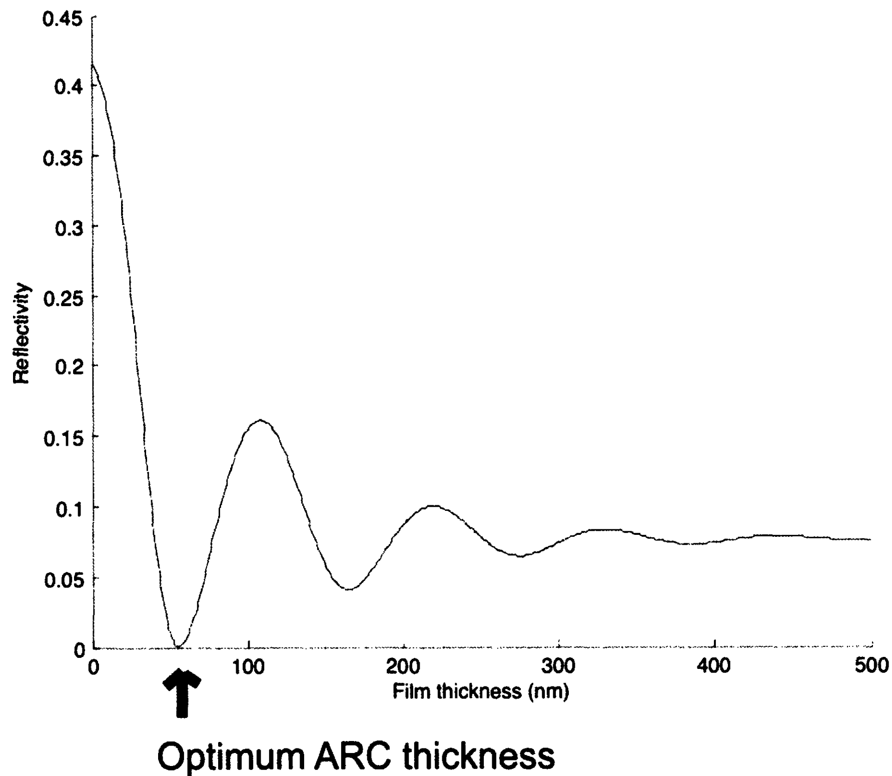

Figure 7: Reflectivity vs XHRIC ARC thickness for 400 nm wavelength with PS4 thickness of 250 nm

This would indicate that the ideal XHRIC thickness is approximately 50 nm. To test this in the lab, we spun up and exposed wafers with varying thicknesses of ARC. XHRIC-16 was spun at 2K, 3K, 4K, 5K, and 6K RPM, and XHRIC-11, a more dilute concentration, was spun at 5K and 6K RPM. These spin speeds correspond to thicknesses of 200, 167 146, 134, 127, 96, and 89 nm, respectively. The spinner was limited to speeds of about 6K RPM, meaning that the thinnest we could spin the XHRIC was about 89 nm. By visually observing the interference fringes, we could ascertain which ARC thickness was the best in reducing the fringes. For the XHRIC-16 (200-127 nm) samples, interference banding was significant, and the variation in thickness very large. For 96 nm thickness, banding was mild, and with 89 nm, almost no banding was observed. The is an explanation for discrepancy between the observed ideal ARC thickness (89 nm) and the prior calculated one (around 50 nm). The thickness of PS4 used in the previous calculation (250 nm) is the thickness measured

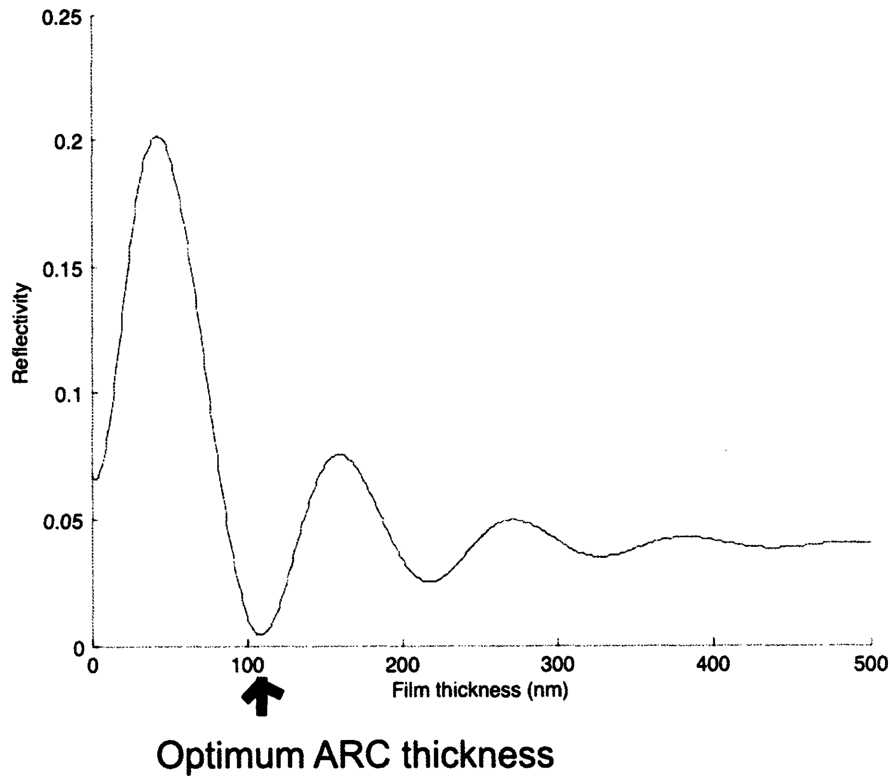

Figure 8: Reflectivity vs XHRIC ARC thickness for 400 nm wavelength with PS4 thickness of 300 nm

after development using the Dektak. In fact, the actual thickness during exposure is approximately 300 nm. Postbaking the resist after exposure causes contraction in the resist, due to the cross-linking of polymer molecules. Therefore, inputting the 300 nm PS4 thickness instead of the 250 nm thickness yields Figure 8, which indeed shows the minimum around the observed thickness of XHRIC.

6 Contrast Measurement Experiments and Results

A large collection of contrast measurements were taken, using exposures on the OAI. At the same time, we sought to tailor the ARC thickness to find the optimal thickness that caused no interference patterns or other optical effects. The general procedure was to spin ARC onto a silicon wafer, then hardbake the wafer to polymerize the ARC.

PS4 photoresist was then spun on, and then baked on a hot plate for 60 seconds at 90 C. The wafer was then exposed in the OAI using the mask we had fabricated. The wafer was then postbaked, usually at 110 C for around 90 seconds. Finally, the wafer was diced into three sections, and developed for 60 seconds in each of the three developer solutions. The three solutions were NaOH with no salt, NaOH with 4% NaCl, and CD26, which is a solution of TMAH. After drying, the thickness of the remaining lines was measured on the Dektak profilometer, and the corresponding thicknesses and optical doses were graphed on MATLAB.

The following figures display the various sets of data obtained. The following graphs display the Resist Thickness Remaining versus Log(Dose). The random error in resist thickness is given as 10 nm, due to roughness in the surface and uncertainty with respect to Dektak profilometer measurements. Due to the fact that our anti-reflection coatings were not perfect, we still suffered from some interference banding and reflections off of our mask. Moreover, while we eventually ascertained the optimal thickness of ARC (as shown in the previous section), quite a few samples were produced with sub-optimal ARC thicknesses, causing interference patterns. These samples are still useful though in observing possible contrast enhancement due to salty development. Thus, each line with a particular dose may have several different thicknesses due to variations in light intensity due to interference effects. Therefore, we decided to display the results for each band separately, rather than show a simple average. Thus, in the following graphs sometimes data for Band 1 and Band 2 is listed; these are the contrast curves derived from measuring the thicknesses of each interference band separately.

Using MATLAB, we used a least-square fitting method to fit the data points to the function in accordance with [10]:

$$RTR = \frac{T}{1+\eta}[(1-e^{-(D-D_0)/A}) + \eta(1-e^{-(D-D_0)/B})] \tag{30}$$

Where T is the original thickness and D_0 is the dose where the resist thickness drops to zero. From there, using this function, we approximated the photoresist contrast as

$$C = \frac{0.75}{log(D_{0.75}) - log(D_0)} \tag{31}$$

Where $D_{0.75}$ is the dose corresponding to 75% resist thickness.

Figure 9 through 14 were exposed with 400 nm light.

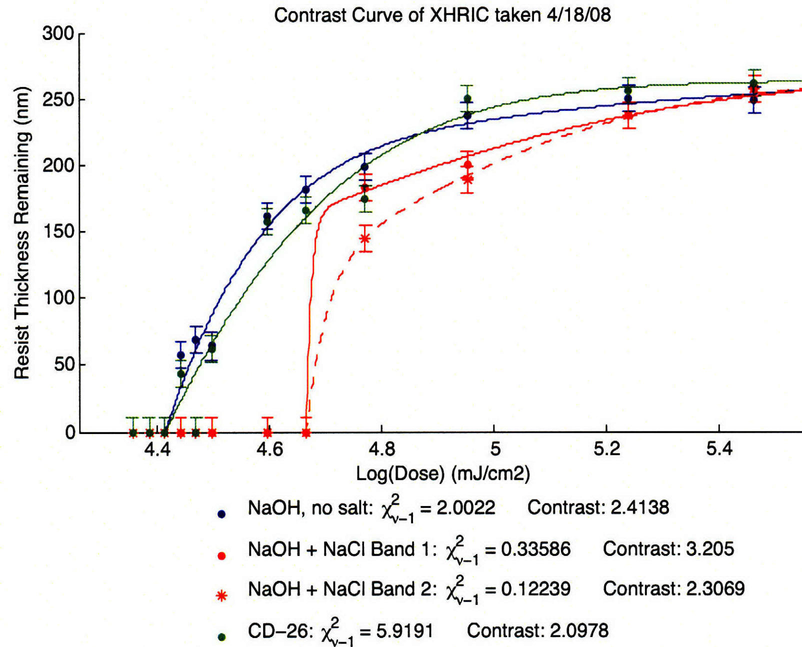

Figure 9: Data Taken 4/18/08: 90 nm XHRIC, baked 175C for 90 seconds, PS4 spun at 1.5K

The data shown in Figures 9 and 10 were taken under similar conditions, both with about 90 nm of XHRIC, identical postbake times, etc. Despite having near the optimal ARC thickness, some interference patterns were still created. From the data, one band developed in salty developer has better contrast than non-salty development, while the other band has about equal contrast. However, due to the small number of data points, it is not clear whether the high contrast for that band is real or an illusion produced by improper curve fitting.

Figures 11 and 12 show data from samples with a sub-optimal thickness of anti-reflection coating, causing multiple interference bands. As can be seen, non-salty development clearly has higher contrast than salty development, contrary to our original hypothesis.

Figures 13 and 14 show data for samples that made use of AZ Barli anti-reflection coating instead of XHRIC. As these were early test samples, the ARC thickness is again sub-optimal. Here though, we still see that non-salty development has higher or at least comparable contrast to salty development.

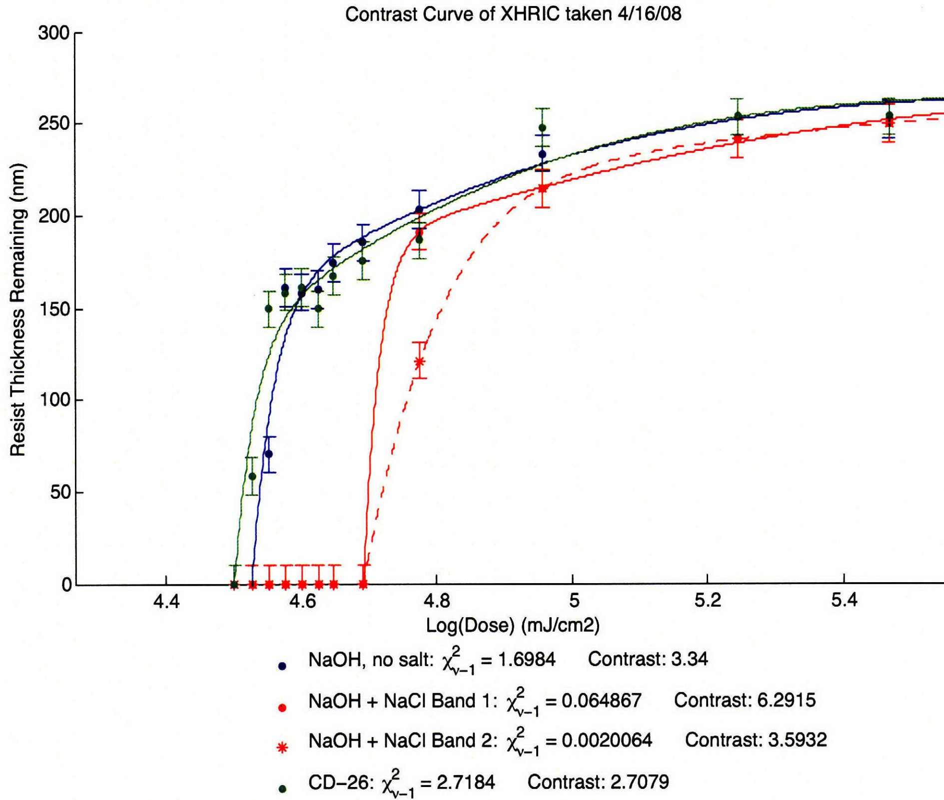

Figure 10: Data Taken 4/16/08: 89 nm XHRIC baked 175C for 90 seconds, PS4 spun at 1.5K

Very early on though, we experimented with 220 nm exposures of PS4, shown in Figures 15 through 17. There were several main problems with exposing at 220 nm, though. First, because of the weak power of the OAI at 220 nm, very long exposures (up to 5 minutes) were required. As a result, we also used weaker developers (0.4% NaOH, 4% NaCl, half-diluted CD-26). However, since researchers and industry typically use full-strength CD-26, we ended up increasing the strength of the developer for later samples; unfortunately, by this time, we had moved on to exposing at 400 nm, and did not end up applying the stronger developers on the 220 nm exposures. In addition, PS4 is designed as a mercury I-line (325 nm) photoresist, and we were unsure of its properties at 220 nm. That being said, the data from the 220 nm

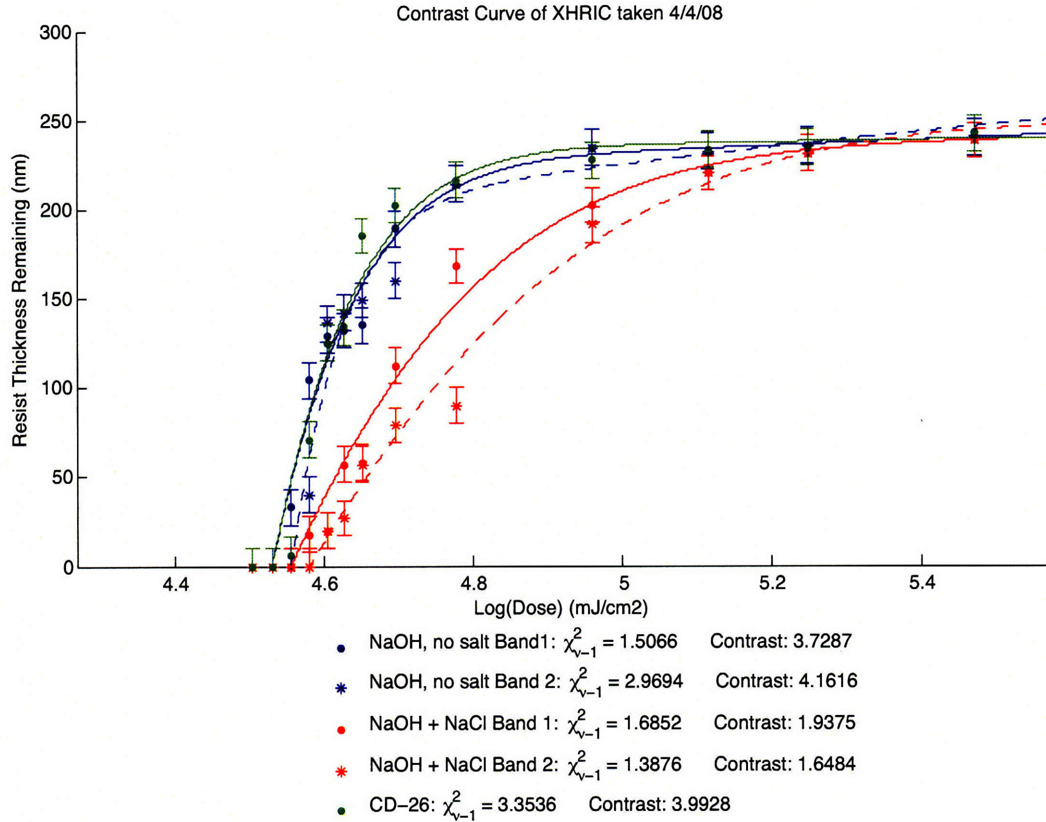

Figure 11: Data Taken 4/4/08: XHRIC-16 spun at 5K, baked 175C for 90 seconds, PS4 spun at 1.5K

exposures indicates that salty development does greatly increase contrast versus non-salty development by a factor of about 2 to 5 times. However, due to using a weaker developer, it is unknown how much of the observed effect is due to the shorter exposure wavelength, and how much is due to the weaker developer.

Moreover, in all of the samples, the dose measured is simply the exposure time multiplied by the incident radiation. However, this is not exactly the amount of energy that is actually absorbed by the resist. Some of the incident power is being reflected, and some is being absorbed by the anti-reflection coating and silicon substrate. Also, due to the previously noted interference effects, the actual light intensity varies along different portions of the exposed lines, meaning that different portions

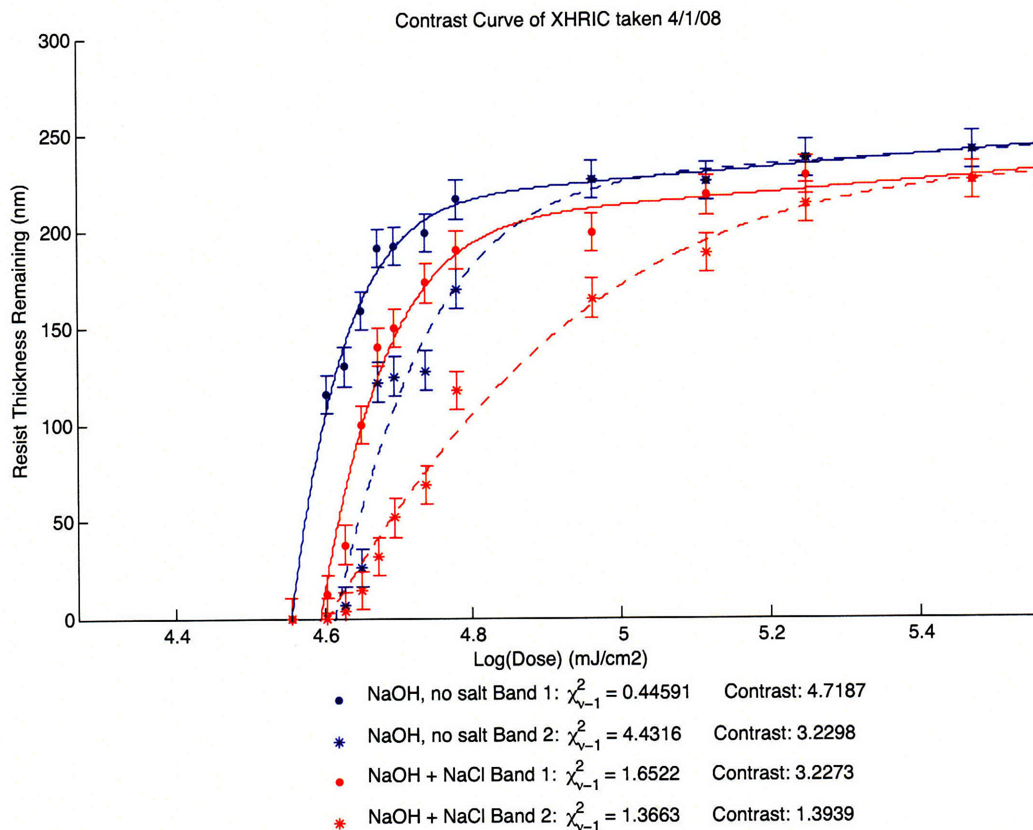

Figure 12: Data Taken 4/1/08: XHRIC-16 spun at 4K, baked 175C for 90 seconds, PS4 spun at 1.5K

of each line absorb different doses. That being said, judging from the reflectivities shown in Figures 7 and 8 (total reflectivity from the setup about 10% at most), it seems reasonable approximating the dose as simply the exposure time multiplied with incident power.

Another observation to be noted is that for all the samples, although contrast enhancement is unclear, salty development increases the dissolution of the resist, as shown by the fact that for all of the samples, for a particular dose, salty development caused greater dissolution than non-salty development.

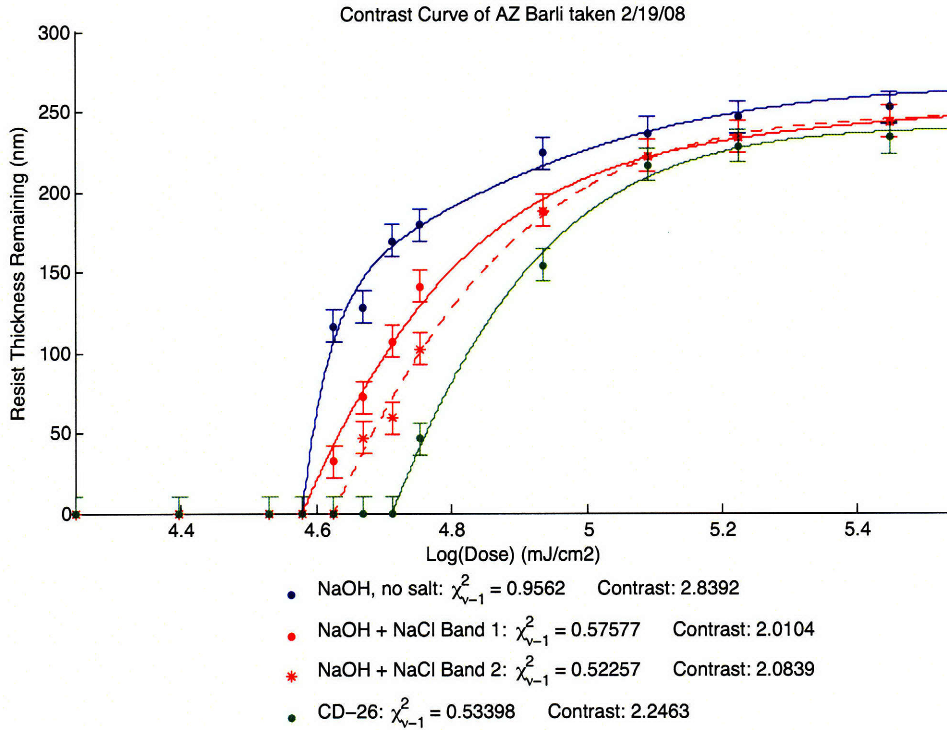

Figure 13: Data Taken 2/19/08: AZ Barli spun at 4K, baked 175C for 90 seconds, PS4 spun at 1.5K, postbake 90 seconds at 110C

7 Discussion

Thus the data for the 400 nm exposed samples generally indicates that salty development has either no effect, or a detrimental effect of photoresist contrast. For 220 nm exposures, however, it seems that salty development increases contrast, however, it is unclear whether the observed effect is more pronounced due to the different formulation of developer. Since the 400 nm samples were developed with a 1:4 ratio of NaOH to NaCl, and the 220 nm were developed with a 1:10 ratio, it is quite possible that the observed effect is more pronounced for 220 nm than 400, so that if we increased the amount of NaCl for the 400 nm developer, we might see more pronounced contrast enhancement.

That being said, it is also highly possible that exposing at 220 nm is necessary to see contrast enhancement due to salty development. Information provided by the

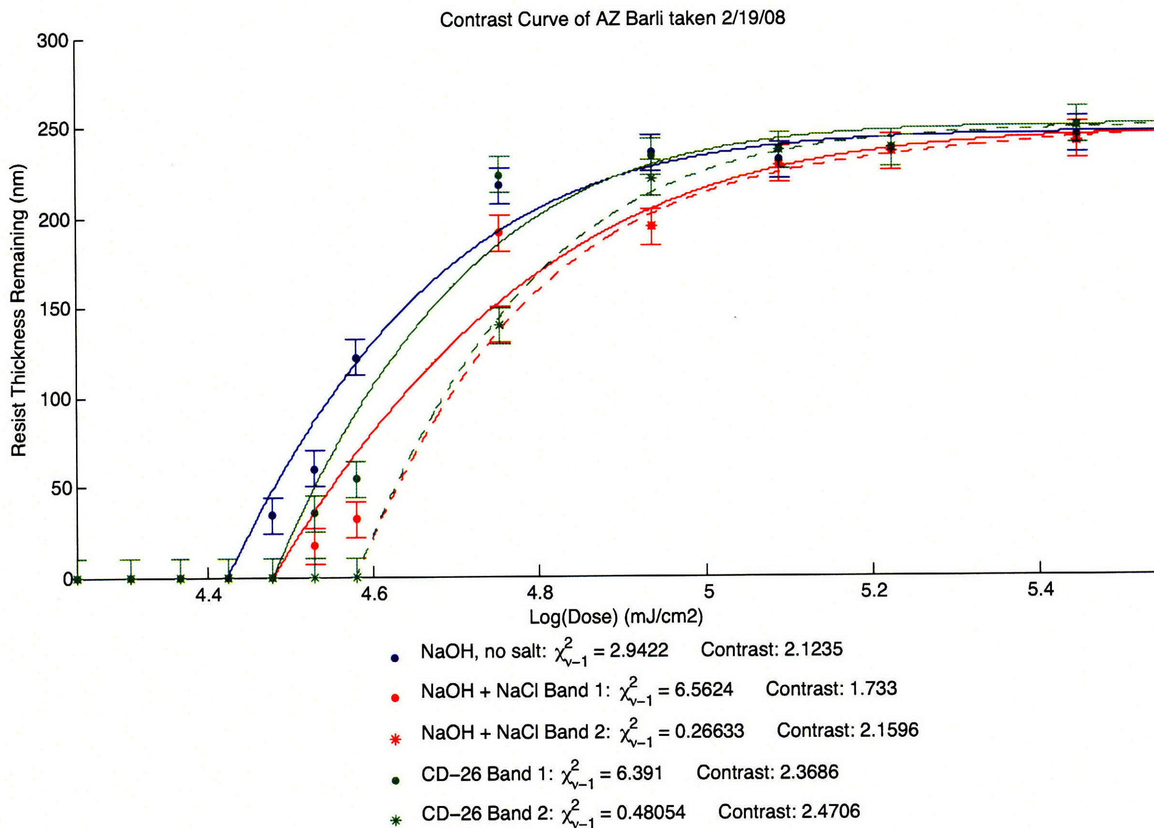

Figure 14: Data Taken 2/19/08: AZ Barli spun at 4K, baked 175C for 90 seconds, PS4 spun at 1.5K, postbake 120 seconds at 110C

MIT Nanostructures Laboratory gives a refractive index of PS4 of 1.667 - 0.016i at 351 nm, 1.681 - 0.016i at 325 nm and 1.395 - 0.747i at 193 nm. This indicates that the absorptivity of PS4 (represented by the imaginary portion of the refractive index) jumps dramatically around 200 nm. This probably indicates a molecular resonance around the 200 nm wavelength. It seems likely this is a resonance in the polymer molecules, not the photoacid generator, since the photoacid generator comprises only a small portion of the resist and already has high absorptivity. Thus, 220 nm light might be ideally suited to directly cross-linking PS4 polymer molecules, something that 400 nm photons might not be able to do.

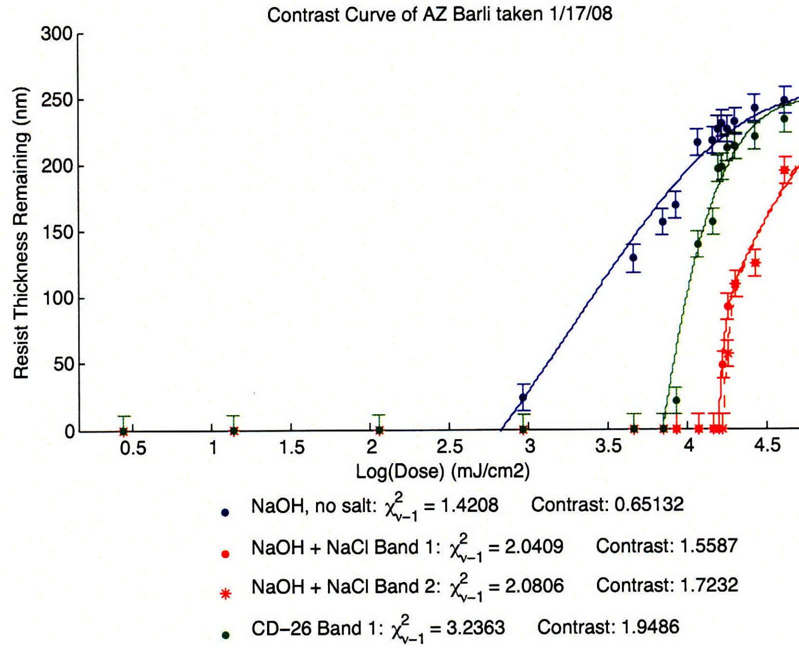

Figure 15: Data Taken 1/17/08: AZ Barli spun at 4K, baked 175C for 90 seconds, PS4 spun at 1.5K, exposed at 220 nm, developed for 60 seconds (NaOH 0.4%, CD26 50% diluted with water)

Cross-linking is invariably related to the dissolution rate of the resist. In experiments with positive-tone resists, the alkaline developer ionizes polymer molecules [9]. This creates negative surface charges which deplete the surrounding area of hydroxide ions, reducing the dissolution rate. The addition of salt has the effect of Debye electrostatic screening of these surface charges, allowing the hydroxide ions to work unhindered.

Debye screening in an electrolytic solution is generally expressed as a length:

$$\kappa^{-1} = \sqrt{\frac{\epsilon_0 \epsilon_r kT}{N_A e^2 \sum C_{\mathrm{B}} Z_{\mathrm{B}}^2}} \tag{32}$$

Where C_{B} is the molar concentration of ionic species B with charge Z_{B}. The ionic species in the solution includes both the added salt and the hydroxide ions [2]. N_{A} is Avogradro's number. Thus, increasing salt concentrations and/or increasing base

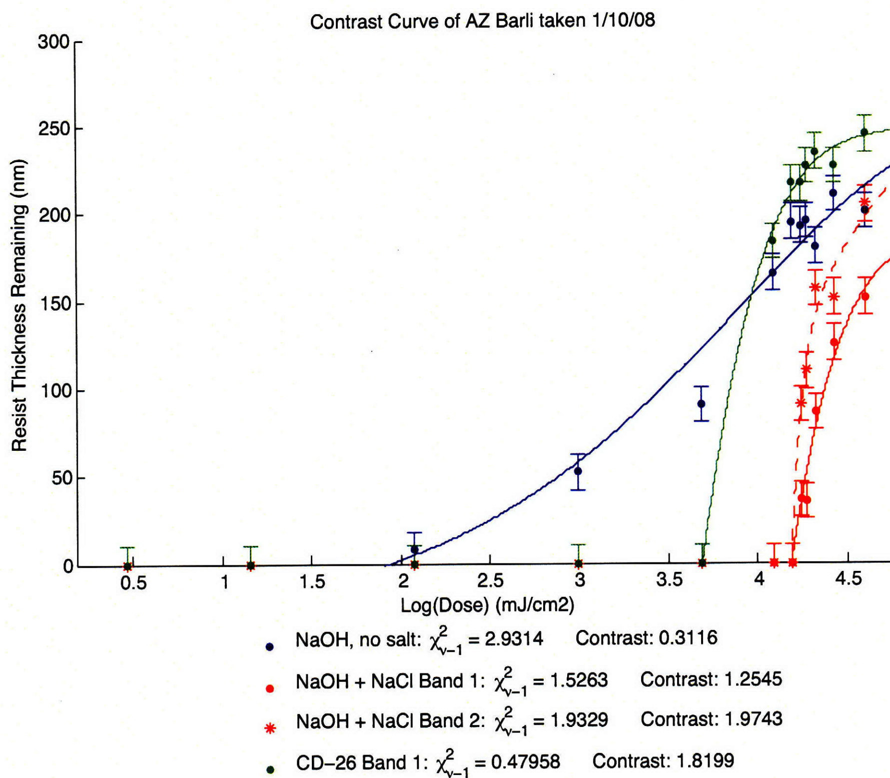

Figure 16: Data Taken 1/10/08: AZ Barli spun at 4K, baked 175C for 90 seconds, PS4 spun at 1.5K, exposed at 220 nm, 90 second postbake, developed for 60 seconds (NaOH 0.4%, CD26 50% diluted with water)

concentration decreases the screening length.

Something similar to this might be at work with PS4. Although contrast enhancement is uncertain, we definitely see increased dissolution due to salty development, which fits well with the idea that the salt is increasing the hydroxide ion reactions. Contrast might then be enhanced because of nonlinear effects involving screening. For instance, the critical ionization model holds that polymer dissolution only occurs when the fraction of ionized monomers reaches a critical value [9]. Screening by salt molecules might affect the fraction of ionized monomers and thereby affect the dissolution rate of the resist.

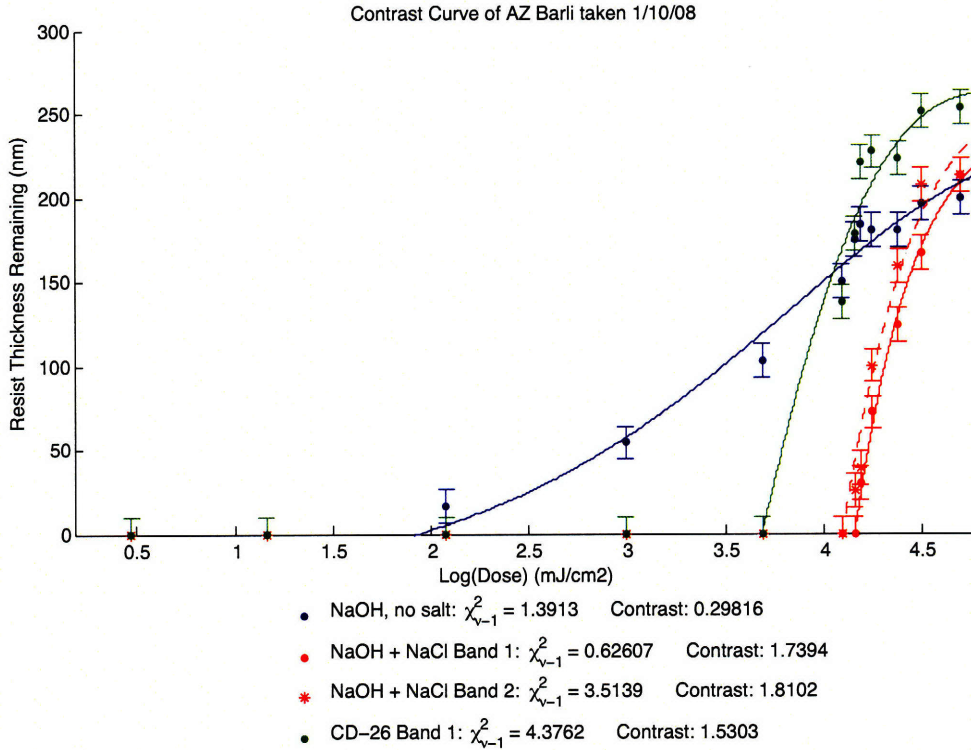

Figure 17: Data Taken 1/10/08: AZ Barli spun at 4K, baked 175C for 90 seconds, PS4 spun at 1.5K, exposed at 220 nm, 120 second postbake, developed for 60 seconds (NaOH 0.4%, CD26 50% diluted with water)

8 Conclusion

8.1 Key Results

In conclusion, we experimented with altering the salt content of photoresist developers, and observed the effect on subsequent photoresist contrast. Problems involving reflections between the mask and photoresist necessitated tailoring an anti-reflection coating, and the optimal ARC thickness was eventually found, agreeing with electromagnetic theory. Measuring the contrast for different developers, we do not find any contrast enhancement through salty development for samples exposed at 400 nm, but we do see an increase in contrast for samples exposed at 220 nm. However, it remains

unclear whether this is due to the shorter wavelength, or a weaker developer that was used for the 220 nm samples.

8.2 Future Work

Future work will invariably involve experimenting more with 220 nm exposures. We also want to experiment with different types of photoresists, both positive and negative. In addition, more research is required to better understand the mechanisms, such as Debye screening, that play a role in photoresist development.

References

[1] Mit 6.152j lecture 10, 2003.

[2] Prabhu et al. Polyelectrolyte effects in model photoresist developer solutions. *J. Vac. Sci B*, 21(4), July 2003.

[3] David Griffiths. *Introduction to Electrodynamics (3rd Edition).* Benjamin Cummings, 1999.

[4] Virginia Semiconductor Inc. Optical properties of silicon- www.virginiasemi.com.

[5] Jin Au Kong. *Electromagnetic Wave Theory.* John Wiley and Sons, 1986.

[6] MIT Nanostructures Laboratory. Ellipsometer sop- stellar.mit.edu.

[7] MIT Nanostructures Laboratory. Index of refraction of il materials- stellar.mit.edu.

[8] Semiconductor Technology Library. 365 nm wavelength arc products- semiconductor.firstlightera.com.

[9] et al Schmid. Electrostatic effects during dissolution of positive tone photoresists. *J. Vac. Sci. B*, 20(6), November/December 2002.

[10] Joel Yang and Karl Berggren. Using high-contrast salty development of hydrogen silsequioxane for sub-10-nm-half-pitch lithography. *EIPBN 2007.*

[11] Peter Van Zant. *Microchip Fabrication, Fifth Edition.* McGraw-Hill, 2004.